From Eötvös to mGal

Study Team 2 – Workpackage 1

The space-wise approach - Overall scientific data strategy

FINAL REPORT

April 10, 2000

A. Albertella, F. Migliaccio, F. Sansó
DIIAR, Politecnico di Milano

C.C. Tscherning
University of Copenhagen, Dept. of Geophysics

Summary

The scope of WP 1 (undertaken by UCPH and POLIMI) was intended as a preparatory work for further studies along the line of the data reduction strategy based on the space-wise approach.

The whole concept of the approach is to use the spatial correlation of the field of the measurements, inherited from the correlation of the anomalous potential, to assemble spatially contiguous observations with the purpose of cross-checking one another and forming spatial (block) averages to be used as observations and having a much lower noise.

The advantage of this approach is to allow comparisons of measurements distant in time but close in space, with a superior capability of controlling biases and to permit the application of anti-aliasing techniques; the disadvantage is a certain difficulty in treating a time-wise colored signal in an optimal way. The method is considered as complementary to the frequency-domain approach, having possibly certain advantages when employed to cross-validate the scientific results.

In this Report, Chapter 1.1 serves as a review of the activities foreseen in the framework of the space-wise approach: it has been prepared mainly by UCPH.

In Chapter 1.2 and Chapter 1.3, two specific problems are studied, namely the comparison of GOCE data with data coming from "sister missions" (which are part of the external information needed for scientific processing) and the check of the operational state of the gradiometer (which is part of the procedures for quality assessment).

Both Chapter 1.2 and Chapter 1.3 regard the work done at POLIMI and have been written by the POLIMI working group. The study described in Chapter 1.2 was presented at IUGG99 in Birmingham.

1.1 Introduction

1.1.1 Definition of the full set of GOCE observations

As a preparation for the implementation of the space-wise approach to GOCE data reduction, we define the full framework of scientific product extraction.

Let us start by defining the observations which can be performed by GOCE.

- Satellite-to-satellite tracking (SST).

  The basic observations are pseudo-ranges and phases of the L1 and L2 signals received from the GPS and GLONASS satellites. A one second sampling is assumed. The mean precision of the pseudo-ranges must be given. (They will probably be constant).

  The positions of the satellites and of GOCE itself must be given (from IGS) in an earth fixed conventional system (CTS), or a similar Earth fixed system valid for a given time period. The positions should be given as Cartesian coordinates with associated standard deviations. The velocity vector of the satellites is also needed.

  The mean error of the quantities must be given. We expect, after a POD procedure is applied, that the satellite position along the orbit be better than 3 cm. Furthermore we expect that by using second phase differences (two positions of the satellite 8 km apart and two GPS or GLONASS satellites) the base vector be estimated at the millimeter accuracy level.

  The data should be tested by forming range rate rates and comparing these rates with directional derivatives of a reference potential, such as EGM96.

- Satellite Gravity Gradiometry (SGG).

  We expect to obtain the inertial tensor ? by differentiation of the accelerometers output. The components will not be point values, but will be filtered mean values along the orbit in a fixed period. The characteristics of the filter must be given (e.g. as weights associated with the time differences). The values must be given in EU with three significant digits.

? must be given in a satellite fixed frame, and the standard error of the filtered values must be given. Along-track correlations must be known or estimated (see [8]).

The data should first be tested by computing anomalous values (i.e. $T_{ij} = V_{ij} - U_{ij}$, where U_{ij} is a reference potential, such as EGM96).

The standard errors of the random signal must be given as calculated from ground based calibrations or cross-over checks.

- Attitude.

  The attitude of the SGG instrument is supposed to be observed by the star-trackers with a precision better than $10''$. The actual mean error must be given. The attitude should make it possible to relate a satellite fixed frame to an earth fixed one.

- Non-gravitational perturbations.

  The vector $\underline{f}_{NG}$ of non-gravitational accelerations can be obtained by adding the accelerometers signal, and it is therefore uncorrelated with ? . The components of $\underline{f}_{NG}$ will be considered as independent and with a m.s.e. equal to $\sigma_{NG} = 1\ nGal/\sqrt{Hz}$.

  One particular problem is that in reality the accelerometers always supply the vector $\underline{f}_{NG}$ in terms of variations with respect to some fixed time, $\underline{f}_{NG} - \underline{f}_{0NG}$; the vector $\underline{f}_{0NG}$ (which can be considered as constant over several revolutions) remains unknown.

1.1.2 Definition of the full set of external information

The external information which will have to be supplied in order to perform the data treatment is given as follows.

- Global digital terrain models.

  In order to improve the reference potential used to compute anomalous values, digital terrain models (DTM) can be used. The global models, however, contain very large errors, which make them very difficult to be used. For regional modelling, however, a regional remove-restore procedure can be used (see [5], [6]). Such models should be given as mean heights of blocks of size $15'$ or smaller (a $5'$ DTM is readily available).

  The use of a DTM can be enhanced using actual densities and depths of compensation. If this information is available, it should be used.

  However, another possibility is to use a first calculated GOCE potential function as a reference function. This would enable a self consistent pre-smoothing of the gravity potential.

- Ground or airborne gravity data.

  These gravity data are essential to reduce biases in the global field estimation when treating the polar gaps problem; in fact it has been proved that including a field of mean gravity data on the polar caps eliminates most of the aliasing generated by the distribution of the data achievable by a satellite like GOCE.

  Moreover, the gravity data will be used in combination with the satellite data in refined regional solutions and for the calibration by upward continuation as described in [7].

  The ground data must be in the GRAVSOFT-standard form (see [23]), i.e.

  identifying number,

  latitude,

  longitude (in decimal degrees),

  altitude (or depth of ocean),

  free-air anomaly or gravity disturbance,

  standard error of the anomaly or disturbance.

  The coordinates must be given in WGS84. The height, however, must be the height above mean sea level for gravity anomalies and ellipsoidal heights for gravity disturbances. The gravity anomaly or disturbance must refer to the IGSN71 system. The error estimate should include the effect of both the coordinate uncertainty and the gravity measurement.

  For the airborne data additional information is needed (see [24]):

  azimuth of flight direction,

  characteristics of the filter used on the raw data.

- Data from sister missions.

  Data from GRACE are basically SST data, and must be treated as such. An analysis should be performed to confirm that GRACE data can be compared with GOCE data only at the level of comparing global solutions. The comparison between the GOCE mission and other missions will be presented in Chapter 1.2.

- Tidal information.

  The tidal forces which are above instrument noise level must be calculated. In general we expect that the tidal effects originating from the Earth will be below noise level.

1.1.3 Frames and interfaces for the treatment of the data

First of all we try to synthetically define the procedure to obtain the Marussi tensor M starting from the inertial tensor ? which, we recall, is known only in its compo-

nents $?_{XX}$, $?_{YY}$, $?_{ZZ}$, $?_{XZ}$ and $?_{ZX}$; therefore all computations are done for these components only.

The chain of SGG estimation can be shortly described as follows.

From ? it is possible to compute the angular acceleration

$$\dot{\omega}_Y = \frac{?_{XZ} - ?_{ZX}}{2} \ . \tag{1.1}$$

By using the observations obtained by the star trackers we can derive ω_Y and finally compute the components of M:

$$\begin{aligned} M_{XX} &= ?_{XX} + \omega_Y^2 \\ M_{YY} &= ?_{YY} \\ M_{ZZ} &= ?_{ZZ} + \omega_Y^2 \\ M_{ZX} &= M_{XZ} = \frac{?_{XZ} + ?_{ZX}}{2} \ . \end{aligned} \tag{1.2}$$

The measurements will be converted to anomalous quantities by linearisation. They may then be represented as the result of a linear functional applied on the anomalous gravity signal, plus systematic effects and random noise. The systematic effects will generally be a bias, plus a quantity linear in time. More difficult problems are out of the scope of the present study.

The noise will be modelled as having a normal distribution with known variance, but with a spatial correlation, along track; or, in a first approximate version, uncorrelated at least for block averaged quantities. This is very important, see [8]. The error correlation has either to be estimated as described in the referenced paper, or calculated based on the observation equations, SST data, for example, will have an along track correlation if represented as range rate rates.

In the simple integration approach data can be used in the above given form, and provide coefficients estimates. This is elementary with the T_{ZZ} component; the $(T_{XX} + T_{YY})$ component is equivalent to the former. Other components are known to provide little incremental information. Regarding this approach, studies are described in [1], [2], [3]. The same approach can be followed at a more advanced level by using suitable sets of functions adapted to the particular observational geometry, like Slepian functions (see [4]).

In the least square collocation method (LSC) the data can be used directly as described above in Section 1.1.2. However, we will have to calculate certain kinds of normal point or "normal area" (means over blocks) values. This is necessary in order to reduce the amount of data (which otherwise cannot be handled globally by LSC). The latter kind of data may readily be used in integration procedures, if for example the normal area values are means of vertical gravity gradient, T_{ZZ}.

1.1.4 Quality control

Different procedures of quality control are possible, and some are already implemented in existing software, such as the GRAVSOFT program GEOCOL.

Moreover new approaches for "loop checks" and cross-over checks will be specifically studied. They will be presented in Chapter 1.3.

However, the simplest control can be made by comparing the satellite data with values calculated from a spherical harmonic model like EGM96. Such a comparison will easily reveal large errors in regions with a smooth gravity field. In mountainous areas, it will be more difficult. But here the existence of a DTM can help to identify high frequency type of errors.

An effective method used on the ground is based on LSC. Each observation is "predicted" from all other data in a certain range. This is already an operational procedure used on airborne gradiometer data (see [8]) and it will be tested on simulated satellite data in WP 3. The identification of systematic errors is also possible using LSC as demonstrated in [7].

1.2 Direct and local comparison between different satellite missions for the gravity field on the flight

1.2.1 Satellite missions for the gravity field

In these days we can perceive a new international effort directed to the determination by spatial means of a reliable model of the gravity field of the earth, based on a set of homogeneous and fairly even distributed observations.

The only drawback is that to measure from space one has to carry an instrument into an orbital altitude which has to be maintained for a suitably long time (e.g. 6 months) at least above the limb of the atmosphere (e.g. about 250 km). Of course this reduces the power of the signal to be measured, namely the gravity field, due to the natural attenuation of harmonic functions inside their domain.

In an effort to capture as much information as possible from measurements, different strategies combining the lowermost orbits with various types of observations have been proposed and are under development, like CHAMP, GRACE and GOCE [13]. With such a wealth of measurements spread in space, we will be able to compute several different models of the gravity field, which therefore will have to be compared to one another, and the question arises whether we could or not directly compare and cross-check observations in space by taking advantage of the marked spatial correlation of the gravity field.

According to the present study, it seems that observations made at significantly different altitudes cannot be directly compared with an accuracy acceptable with respect to measurement noise, nevertheless observations at the same altitude can be used to "self calibrate" the instruments when the satellite passes over the same area at different times.

This is most easily done when the direct observations are first preprocessed in order to produce intermediate observables which are expressed by "local" functionals of the gravity field, which can then be treated in the manner of a boundary value problem (globally) or of the collocation concept (locally).

1.2.2 Space observations and their localization

When reasoning only on the feasibility of a direct comparison of observations we can in principle start with a very simplified model. Working with mission "M", we can write the equation of the reference orbit as

$$\ddot{\underline{\tilde{x}}}_M = \nabla u_0(\underline{\tilde{x}}_M) \tag{1.3}$$

where u_0 represents the known model potential.

Hill's perturbation equations of motion are written as

$$\ddot{\underline{\xi}}_M + 3n_M^2(I - 3P_r)\underline{\xi}_M = \nabla T(\underline{\tilde{x}}_M) + \underline{f}_p \tag{1.4}$$

n being the mean motion of the satellite, $\underline{f}_p$ the perturbation forces acting on the satellite (both non-gravitational and gravitational) and P_r a radial projection operator.

Tracking or in situ observations in their linearized form can be represented as [12]

$$\begin{aligned} Q_t &= F_t(\underline{x}_M; \dot{\underline{x}}_M; T) = \\ &= \tilde{Q}_t + K^+_{Mt}\underline{\xi}_M(t) + H^+_{Mt}\dot{\underline{\xi}}_M(t) + L_{Mt}(T) \end{aligned} \tag{1.5}$$

where $\underline{\xi}(t)$ and $\dot{\underline{\xi}}(t)$ represent the orbit anomaly and its time derivative,

$$\begin{aligned} \begin{vmatrix} \underline{\xi}_M(t) \\ \dot{\underline{\xi}}_M(t) \end{vmatrix} &= \begin{vmatrix} F_t \\ \dot{F}_t \end{vmatrix} \cdot \begin{vmatrix} \underline{\xi}_M(0) \\ \dot{\underline{\xi}}_M(0) \end{vmatrix} + \\ &+ \int_{(\underline{\tilde{x}}_M)}^{t} \begin{vmatrix} G(t,\tau) \\ \dot{G}(t,\tau) \end{vmatrix} \cdot \nabla T(\underline{\tilde{x}}_M(\tau))d\tau \end{aligned} \tag{1.6}$$

Localization can be achieved by inspecting the observation equations and suitably exploiting Hill's equations in such a way as to eliminate the need of the orbital parameters $\underline{\xi}_0, \dot{\underline{\xi}}_0$ corresponding to initial data.

In the following we will specify Eq. (1.5) for the different cases of observation strategies under development.

- High-Low SST (CHAMP)

  The observations are represented by

$$\underline{Q}_t = \underline{x}_t = \underline{\tilde{x}}_t + \underline{\xi}_t \tag{1.7}$$

  The stochastic order of magnitude (SO), which can be defined through the root mean square of random variables in analogy to the O of Landau, for the observed values of $\underline{\xi}_t$ is given by [10]

$$SO(\underline{\xi}_t) \sim 1\ cm \quad . \tag{1.8}$$

  Moreover, bases joining two observation points can be observed with higher precision, for instance $SO \sim 0.5\ cm$.

  If we now make the hypothesis that the time interval between observations is $\Delta t = 10\ s$, which gives a distance along the orbit arc of about 100 km, having

$$\frac{\underline{\xi}_{t+2\Delta t} + \underline{\xi}_t - 2\ \underline{\xi}_{t+\Delta t}}{(\Delta t)^2} \sim \underline{\ddot{\xi}} \tag{1.9}$$

  we obtain

$$SO(\underline{\ddot{\xi}}) \sim 10^{-2}\ cm\ s^{-2} = 5\ mGal \tag{1.10}$$

$$SO(n^2\ \underline{\xi}) \sim 10^{-3}\ cm\ s^{-2} = 1\ mGal \tag{1.11}$$

  Filters can be applied to recover 0.5 $mGal$ along the orbit [9].

- Low-Low SST (GRACE)

  For this mission, three kinds of observations must be taken into account, and their corresponding SO [10]:

  a) by GPS observations, considering that the satellite passes from position 1 to position 2 in $\Delta t = 10\ s$ we have

$$\underline{Q}_t = \underline{x}_2 - \underline{x}_1 = \underline{\tilde{x}_2} - \underline{\tilde{x}_1} + \underline{\xi}_2 - \underline{\xi}_1 \tag{1.12}$$

$$SO(\underline{\xi}_2 - \underline{\xi}_1) \sim 5\ mm \tag{1.13}$$

  which is practically the same kind of observable discussed in the previous part for CHAMP;

  b) by distance observations we have

$$Q_t = |\underline{x}_2 - \underline{x}_1| = \tilde{Q}_t + \underline{\tau} \cdot (\underline{\xi}_2 - \underline{\xi}_1) \tag{1.14}$$

where $\underline{\tau}$ represents the unit vector in the along track (tangential) direction to the orbit, hence the index τ will denote this direction;

$$\begin{aligned} SO(\xi_{2\tau} - \xi_{1\tau}) &\sim 5 \cdot 10^{-2}\ mm \\ SO(\ddot{\xi}_{2\tau} - \ddot{\xi}_{1\tau}) &\sim \frac{\sqrt{2} \cdot 5 \cdot 10^{-2}}{\Delta t^2} = \\ &= 10^{-4}\ cm\ s^{-2} = \\ &= 0.1\ mGal \end{aligned} \tag{1.15}$$

c) by Doppler observations we have

$$Q_t = \frac{\partial}{\partial t}|\underline{x}_2 - \underline{x}_1| = \tilde{Q}_t + \dot{\xi}_{2\tau} - \dot{\xi}_{1\tau} \tag{1.16}$$

which combined with the difference of the radial components $(\xi_{2r} - \xi_{1r})$ in Hill's equations gives

$$\ddot{\xi}_\tau + 2n\dot{\xi}_r = \underline{\tau} \cdot \nabla T \tag{1.17}$$

The following stochastic orders of magnitude are expected

$$\begin{aligned} SO(\dot{\xi}_{2\tau} - \dot{\xi}_{1\tau}) &\sim 5\ 10^{-3}\ mm\ s^{-1} \\ SO\left(\frac{\dot{\xi}_{2\tau} - \dot{\xi}_{1\tau}}{\Delta t}\right) &\sim 5\ 10^{-4}\ mm\ s^{-2} \\ SO\left(n\ \frac{\xi_{2r} - \xi_{1r}}{\Delta t}\right) &\sim 1\ \mu Gal \\ SO(\underline{\tau} \cdot \nabla T) &\sim 50\ \mu Gal \end{aligned} \tag{1.18}$$

- Gravity Gradiometry (GOCE)

  The observations are represented by [14]

$$Q = M \equiv \left[\partial^2_{ik} T\right] \tag{1.19}$$

  In this case it must be noticed that Q has the great advantage of being always localized.

  The stochastic order of magnitude of M is given by

$$SO(M) \sim 10^{-12}\ s^{-2} \quad . \tag{1.20}$$

1.2.3 Comparison between spatially distributed observations coming from different missions

In this section we will consider two cases: first we will show how to compare gravity models derived from different satellite missions (with a testing procedure); afterwards we will discuss the problem of predicting one observable from another of a different kind and we will produce an elementary, yet meaningful, example.

1.2.3.1 Comparison of derived gravity field models

In this case we want to compare the estimated coefficients of model (1) with the estimated coefficients of model (2), which in general have been estimated using data coming from different missions and have different resolutions:

$$\begin{aligned} \hat{T}^{(1)}_{nm} \;&\Rightarrow\; \underline{\hat{T}}^{(1)}_{m} = \left\{ T^{(1)}_{nm} \;,\; n = m, \ldots, N^{(1)} \right\} \\ \hat{T}^{(2)}_{nm} \;&\Rightarrow\; \underline{\hat{T}}^{(2)}_{m} = \left\{ T^{(2)}_{nm} \;,\; n = m, \ldots, N^{(2)} \right\} \end{aligned} \tag{1.21}$$

We will use the symbols $C^{(1)}_m, C^{(2)}_m$ to represent the covariance matrices of the coefficients, order by order. In fact it must be noticed that typically correlations exist among estimated coefficients with different degree but same order. A testing procedure can be established as follows. Under the hypothesis that $N^{(2)} > N^{(1)}$, a projection must be performed of $\underline{\hat{T}}^{(2)}_m$ on $\underline{\hat{T}}^{(1)}_m$

$$\Pi_{21}\; \underline{\hat{T}}^{(2)}_m = \underline{\hat{T}}^{(21)}_m \quad ,\; n = m, \ldots, N^{(2)} \tag{1.22}$$

Introducing the covariance of the $(N^{(1)} - m)$ components of $\underline{\hat{T}}^{(2)}_m$, $C^{(21)}_m$, we can write

$$\Pi_{21}\; C^{(2)}_m\; \Pi^{+}_{21} = C^{(21)}_m \tag{1.23}$$

and finally set the test

$$\begin{aligned} &\left[\underline{\hat{T}}^{(21)}_m - \underline{\hat{T}}^{(1)}_m \right]^{+} \left[C^{(1)}_m + C^{(21)}_m \right]^{-1} \left[\underline{\hat{T}}^{(21)}_m - \underline{\hat{T}}^{(1)}_m \right] = \\ &\qquad = \chi^2_{(N^{(1)} - m)} \end{aligned} \tag{1.24}$$

which holds if

$$H_0 \;:\; E\{\underline{\hat{T}}^{(21)}_m\} = E\{\underline{\hat{T}}^{(1)}_m\} \tag{1.25}$$

is satisfied.

1.2.3.2 Prediction of one observable from another

The direct prediction by collocation of one spatial observable from another between very different altitudes not only when going downward, but even when going upward

by some 100 km, seems to be unable to recover the level of a very accurate local measurement.

Here we will discuss an example. Let us take one observation of the second radial derivative T_{zz} at a point P at an altitude of 250 km and try to predict the first radial derivative T_z at a point Q at an altitude of 400 km along the same radius.

Setting $U_0 = \frac{\mu}{R}$ we can write the usual formula for the gravity potential

$$T = U_0 \sum_{N_{min}}^{N_{max}} T_{nm} \left(\frac{R}{r}\right)^{n+1} Y_{nm} \tag{1.26}$$

$$O(T_{nm}) = \frac{10^{-5}}{n^2} \quad \text{(Kaula's rule)}$$

The covariance function of the gravity potential can be written as

$$\begin{aligned} & C_{TT}(P,Q) = \\ & = U_0^2 \sum_{N_{min}}^{N_{max}} \left(\frac{R^2}{r_P r_Q}\right)^{n+1} \sigma_n^2 (2n+1) P_n(t) \\ & (t = \cos\psi) \end{aligned} \tag{1.27}$$

where σ_n^2 is the variance of the individual coefficient, hence $(2n+1)\ \sigma_n^2 = C_n$ represents the degree variance (full power),

$$C_n = \frac{2n+1}{n^4}\ 10^{-10} \sim \frac{2\ 10^{-10}}{n^3} \quad .$$

The first derivative of the potential and its covariance function are (setting $?_0 = \frac{\mu}{R^2}$)

$$\delta g = T_z = -?_0 \sum_{n,m} T_{nm}(n+1) \left(\frac{R}{r}\right)^{n+2} Y_{nm} \tag{1.28}$$

$$\begin{aligned} & C_{\delta g \delta g}(P,Q) = \\ & = ?_0^2 \textstyle\sum_n C_n (n+1)^2 \left(\frac{R^2}{r_P r_Q}\right)^{n+2} P_n(t) \end{aligned} \tag{1.29}$$

The second derivative of the potential, the cross-covariance between δg and T_{zz} and the covariance of T_{zz} are (setting $G_0 = \frac{\mu}{R^3}$)

$$T_{zz} = G_0 \sum_{n,m} (n+1)(n+2) T_{nm} \left(\frac{R}{r}\right)^{n+3} Y_{nm} \tag{1.30}$$

$$C_{\delta g T_{zz}}(P,Q) \;=\; -?_0 G_0 \sum_n C_n (n+1)^2 (n+2) \cdot$$
$$\cdot \left(\frac{R}{r_P}\right)^{n+2} \left(\frac{R}{r_Q}\right)^{n+3} P_n(t) \tag{1.31}$$

$$C_{T_{zz}T_{zz}}(P,Q) =$$
$$= G_0^2 \sum_n C_n (n+1)^2 (n+2)^2 \left(\frac{R^2}{r_P r_Q}\right)^{n+3} P_n(t) \tag{1.32}$$

The prediction of T_z at point Q starting from the observed value of T_{zz} at point P can then be achieved by the formula

$$\hat{T}_z(Q) = C_{\delta g T_{zz}}(Q,P)\; C^{-1}_{T_{zz}T_{zz}}(P,P)\; T_{zz}(P) \tag{1.33}$$

and the mean square error of the prediction is represented by

$$\begin{aligned} \mathcal{E}^2 \;&= C_{\delta g \delta g}(Q,Q) + \\ &- C_{\delta g T_{zz}}(Q,P)\; C^{-1}_{T_{zz}T_{zz}}(P,P)\; C_{T_{zz}\delta g}(P,Q) \end{aligned} \tag{1.34}$$

An easy computation leads to the following formula for $\mathcal{E}^2$

$$\mathcal{E}^2 = \; 2\; 10^{-10}\; ?_0^2 \cdot$$
$$\cdot \left\{ \sum_n \tfrac{1}{n} (q^2)^{n+2} - \frac{\left[\sum p^{n+3}\; q^{n+2}\right]^2}{\sum n (p^2)^{n+3}} \right\} \tag{1.35}$$

where $q = \frac{R}{r_Q},\; p = \frac{R}{r_P}$.

The numerical evaluation of (1.35) for $N_{min} = 10,\; N_{max} = 200$ gives

$$\mathcal{E} = 2.206\; mGal \quad .$$

A remark has to be made: roughly speaking, based on this elementary example we can say that this kind of prediction cannot for instance be used to check the fine Doppler GRACE observations by GOCE observations. Nevertheless it could be used to check the GPS tracking (CHAMP and GOCE).

Of course one could argue that this figure does not justify that the direct cross-control can be applied to the two missions, because the computation has been performed for one measurement only. However, even considering 100 measurements we would reduce the error by a factor 10 if the prediction error had been white noise, what is not, because the collocation error is very correlated. Then even a figure like 0.2 $mGal$ would not be enough to perform the sought check.

1.2.4 Self calibration of a mission

In this section we will compare two observables of the same kind under two different hypotheses, namely: the observables are taken on parallel orbits laying at the same altitude, and the observables are taken on crossing orbits almost at the same altitude.

1.2.4.1 Comparison of two observables of the same kind on parallel orbits at the same altitude

Again, we want to discuss an example consisting in making the simple prediction at one point starting from a single observation, as discussed before. Let us take one observation of the second radial derivative T_{zz} at a point P along an orbit arc at 250 km and let us predict the value of T_{zz} at a point Q along an orbit arc laying at the same altitude, at an (angular) distance from the first arc equal to ψ. In this case we have $\frac{R}{r_P} = \frac{R}{r_Q} = q$ and the prediction error is represented by

$$\begin{aligned} \mathcal{E}^2 &= C_{T_{zz}T_{zz}}(Q,Q) - \frac{C^2_{T_{zz}T_{zz}}(P,Q)}{C_{T_{zz}T_{zz}}(P,P)} = \\ &= 2\ 10^{-10} G_0^2 \cdot \\ &\cdot \frac{\left[\sum_n n(q^2)^{n+3}\right]^2 - \left[\sum_n n(q^2)^{n+3} P_n(t)\right]^2}{\sum_n n(q^2)^{n+3}} \end{aligned} \tag{1.36}$$

The numerical evaluation of (1.36) for $N_{min} = 10,\ N_{max} = 200$ gives

$$\begin{aligned} \mathcal{E} &= 0.024\ E \quad \text{for} \quad \psi = 0.25^\circ \\ \mathcal{E} &= 0.012\ E \quad \text{for} \quad \psi = 0.125^\circ \end{aligned} \tag{1.37}$$

The angular distance $\psi = 0.25^\circ$ between two tracks will be certainly attained after 6 months of observations.

It must be remarked that the *same* computation holds for the prediction from one observation to the other along the orbit, although in this case *real* observations are even much closer to one another.

1.2.4.2 Comparison of two observables of the same kind on orbits crossing at almost the same altitude

It often happens that ascending and descending orbits cross at almost the same altitude. In this case radial derivatives can be directly compared for both GRACE and GOCE missions. We will produce two examples corresponding to the two cases.

a) GRACE

We consider the T_z observations derived from GPS and accelerometers. We want to determine whether we can simply write

$$T_z(P) \cong T_z(Q) \tag{1.38}$$

when the two points P, Q are on the same radius at distance

$$\delta r \leq 10 \ km \quad ,$$

which is not a very stringent condition.
The relation (1.38) can be accepted if

$$SO(T_{zz}) \cdot 10 \ km < \sigma_{noise} \quad .$$

We have

$$\begin{aligned} SO(T_{zz})^2 \ &= 2 \ 10^{-10} \ G_0^2 \sum_n n(q^2)^{n+3} = \\ &= 2 \ 10^{-10} \ G_0^2 \ F(q^2) \end{aligned} \tag{1.39}$$

For $N_{min} = 10, \ N_{max} = 200$, it is $F(q^2) \cong 32$, therefore

$$SO(T_{zz})^2 \sim 64 \ 10^{-10} \ G_0^2 \quad .$$

In the end we obtain

$$SO(T_{zz}) \cdot 10 \ km \sim 0.12 \ mGal \tag{1.40}$$

which shows that we can at least control the radial derivative $\delta g \sim T_z$.

b) GOCE

In this case we want to verify the applicability of the control test

$$T_{zz}(P) \cong T_{zz}(Q) \tag{1.41}$$

when P, Q are on the same radius at distance

$$\delta r \leq 1 \ km \quad .$$

Orbit simulations of the GOCE mission show that this condition is met at least twice per cycle.
In this case it is possible to demonstrate both analytically and numerically that

$$SO(T_{zzz}) \sim 1.24 \ 10^{-15} \ s^{-2} \ m^{-1}$$

therefore for a radial distance between two crossing orbits smaller than 1 km one has

$$SO(T_{zzz}) \cdot 1km \simeq 1.24 \ 10^{-12} \ s^{-2}$$

showing that it is possible to test in this way the functionality of the (zz) channel of the gradiometer, since $SO(T_{zzz}) \cdot 1 \ km$ is smaller than the measurement noise.

1.2.5 Conclusions

The conclusions that we can draw can be summarized as follows.

Regarding the cross checking of the observations taken from two different missions, it seems evident that in general the prediction of one observable from another of a different kind is not feasible, even when going upward. The only possible use could be the control of GPS - accelerometric observations from gradiometric measurements. Of course, it is always possible to compare two gravity potential models obtained from observations of different satellite missions in terms of their coefficients, using a χ^2 test, introducing suitable covariance matrices for the coefficients of the two models.

Regarding the so called "self calibration", it means that observables of the same kind coming from the same mission are compared by predicting the value at one point starting from the value observed at a different point. It is possible to check observations taken at cross-over points, i.e. at points having the same geographic coordinates but laying on crossing orbits at different altitudes. In particular, for GOCE it is possible to predict values of T_{zz} at cross over points with a maximum distance of 1 km in altitude, thus establishing a control test. The feasibility of this test has also been numerically controlled for series of points providing results in the expected range.

1.3 Checking the GOCE gradiometer on the flight by use of loops, cross-overs and overlapping tracks

1.3.1 Check of the operational state of the gradiometer

The purpose of this report is to study tools which will allow checking the operational state of the GOCE gradiometer on the flight (OTF). In particular we will construct testing procedures, based on suitable combinations of the second derivatives, providing the prediction of a field functional performed at the same point in space from two crossing arcs. The check consists in verifying that the two estimated values lie in an interval of given significance; if one of the observed tensor components used in performing the estimates is affected by a gross (outlying) error, the test will fail and we will know that the particular data set at hand should be re-examined.

As we shall see, there are cases (for instance, every time that a cross-over is produced after 1 cycle only, what we will call a *loop*) when the two crossing arcs are practically in the same altitude (i.e. the height difference produces negligible variations in the tensor components). In these cases the check is quite elementary and it can be realistically performed.

A different situation occurs when the crossing arcs are separated by several kilometers in height (we shall present examples with 15 km height difference). Here too it would

be possible to set up a check with a reasonable significance level, if we could know the (x,y) and (y,z) components with a not too degraded accuracy. Actually this is not the realistic case, yet we think it is interesting to be aware of the argument.

Let us also mention that, beyond the OTF checking of the instrument, the cross-over analysis is likely to be useful in the data treatment chain: for instance it could allow the determination of bias terms or of other parameters which could be considered as constant along one or several arcs.

Finally, if the orbit is exactly repeating, within say 1 km, we can consider pieces of arcs as coinciding, while if it is only the ground track which is repeated and the heights of the orbit arcs are different, we can still set up a useful check on the second order along-track derivative.

1.3.2 The cross-overs and loops geometry

Assume to have two arcs of the GOCE trajectory (A, B) and (A_0, B_0), such that e.g. (A, B) is ascending and (A_0, B_0) is descending, and their projection on the mean earth sphere at a point C' (cf. Fig. 1.1).

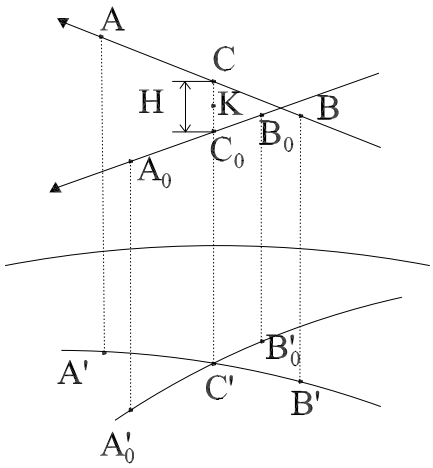

Figure 1.1: The cross-over geometry.

If we assume that (B, A) and (B_0, A_0) are consecutive measurement points, several consequences become evident and quantitatively the geometry of the cross-over is restricted by bounds which we summarize:

- at the rate of 1 measurement per second we have $\overline{AB} = \overline{A_0B_0} = d \cong 8\ km$;
- the height of A, B, A_0, B_0, C, C_0 on the sphere is $\sim 250\ km$;

- the azimuth α of the ascending arc is purely a function of the latitude φ, according to the formula

$$\sin\alpha = \frac{n\dfrac{\cos I}{\cos\varphi} - \omega\cos\varphi}{\sqrt{n^2 + \omega^2\cos^2\varphi - 2n\omega\cos I}} \tag{1.42}$$

where

n = satellite mean motion,

ω = angular velocity of the earth;

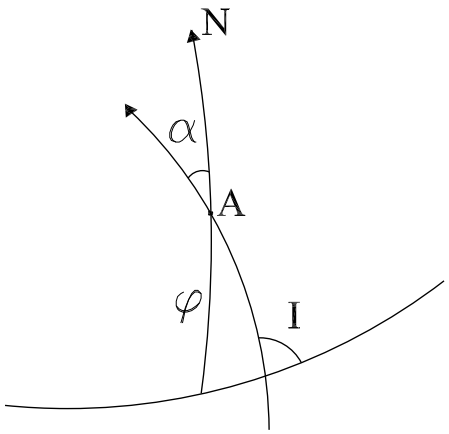

Figure 1.2 : Azimuth of an ascending arc.

- the radius from the center through C' also orthogonally intersects (A, B) in C and (A_0, B_0) in C_0;
- the length of the segment $\overline{CC_0}$, which is orthogonal to both arcs, is the minimum distance $H = \overline{CC_0}$ between the two; H has a maximum amplitude depending on the orbit control manoeuvring and in any case it should amount to a maximum of $2er \sim 26.5\ km$ (e = eccentricity, r = mean orbit radius); in some of the examples hereafter, we shall consider the case

$$\overline{CK} = \overline{KC_0} = \frac{H}{2} = 7.5\ km \quad ; \tag{1.43}$$

- the point C' has then coordinates on the unit sphere such that

$$\underline{r}(C') = \frac{\overrightarrow{BA} \wedge \overrightarrow{B_0A_0}}{|\overrightarrow{BA} \wedge \overrightarrow{B_0A_0}|} = \frac{\overrightarrow{BA} \wedge \overrightarrow{B_0A_0}}{d^2 \sin 2\alpha} \ , \tag{1.44}$$

which indeed can be transformed into $\varphi_{C'}, \lambda_{C'}$;

- one has

$$\begin{cases} \dfrac{AC}{AB} = \dfrac{A'C'}{A'B'} = \lambda \\ \dfrac{A_0C_0}{A_0B_0} = \dfrac{A'_0C'}{A'_0B'_0} = \lambda_0 \end{cases} \tag{1.45}$$

and these two values can be easily computed from the geodetic coordinates of A', B', A'_0, B'_0 which are the same as those of A, B, A_0, B_0;

- one can approximately put

$$H_C = \lambda H_A + (1-\lambda) H_B \ ,$$

$$H_{C_0} = \lambda_0 H_{A_0} + (1-\lambda_0) H_{B_0} \ ,$$

from which one easily computes

$$H = C_0C = H_C - H_{C_0} \tag{1.46}$$

The observed quantities we shall consider are the components of the Marussi tensor, in the instrumental frame,

$$M = \left[\frac{\partial^2 T}{\partial x_i \partial x_k} \right] \quad \text{at } A, B, A_0, B_0 \ ; \tag{1.47}$$

we will specify afterwards the hypotheses on their accuracies.

Furthermore we shall assume that the attitude of the instrument is approximately the same in A and B as well as in A_0 and B_0; moreover the two attitudes will be considered as known to the extent that we can assume to know M in the frames adapted to the two orbital arcs, namely $F \equiv (X, Y, Z)$ with

$\underline{e}_x$ in the $\overrightarrow{BA}$ direction,

$\underline{e}_z$ radial in C [1],

$\underline{e}_y$ to complete the triad,

[1] Rigorously, if we considered $\underline{e}_z$ radial at any other point, it could not be anymore orthogonal to $\underline{e}_x$.

and similarly for $F_0 \equiv (X_0, Y_0, Z_0)$; note that under our hypotheses

$$\underline{e}_z \equiv \underline{e}_{z_0} \quad . \tag{1.48}$$

We conclude these remarks of geometrical nature by observing that the rotation R_0 from the F_0 to the F components can be explicitly given as a function of latitude only, since (1.48) has to hold and by inspection of Fig. 1.3 one easily realizes that

$$R_0 = \begin{vmatrix} -\cos 2\alpha & -\sin 2\alpha & 0 \\ \sin 2\alpha & -\cos 2\alpha & 0 \\ 0 & 0 & 1 \end{vmatrix} \tag{1.49}$$

so that for any vector

$$\begin{aligned} \underline{v} &= v_{x_0} \cdot \underline{e}_{x_0} + v_{y_0} \cdot \underline{e}_{y_0} + v_z \cdot \underline{e}_z \equiv \\ &\equiv v_x \cdot \underline{e}_x + v_y \cdot \underline{e}_y + v_z \cdot \underline{e}_z \end{aligned}$$

one has

$$\begin{vmatrix} v_x \\ v_y \\ v_z \end{vmatrix} \equiv R_0 \begin{vmatrix} v_{x_0} \\ v_{y_0} \\ v_{z_0} \end{vmatrix} \quad . \tag{1.50}$$

As we know, likewise, a tensor as M will be transformed in such a way that

$$M = R_0 M_0 R_0^+ \quad . \tag{1.51}$$

Now the quantities to be tested at K are computed under the basic assumptions that in the small volume delimited by the tethraedron (A, B, A_0, B_0) all field quantities vary linearly in the $\underline{e}_x, \underline{e}_{x_0}$ directions as well as in the $\underline{e}_z$ direction.

Remark 1

The above is indeed a very simplistic hypothesis, however it proves to be perfectly legitimate due to the fact that the distances involved are short. This could not be substituted easily by more refined theories, like least squares collocation, without an accurate local evaluation of the empirical covariances. Then our approach is both realistic and easy to be numerically implemented.

Remark 2

When $(A, B), (A_0, B_0)$ are separated by (approximately) one revolution we call C, C_0 loop points. We claim that $|H| = |H_C - H_{C_0}| < 100\ m$.

In fact first of all the drag compensation on the GOCE satellite will tend to contrast the loss of potential energy, i.e. the fall due to the drag, to the extent

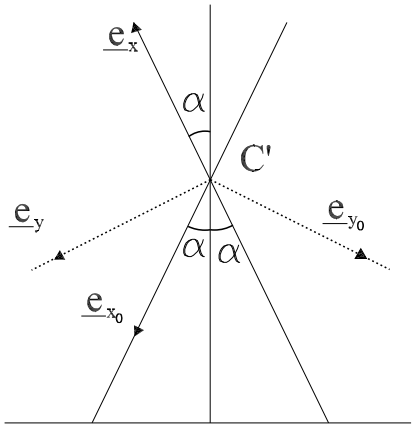

Figure 1.3: Geometry of the rotation $F_0 \to F$..

that we can assume this effect to be of the order of meters. So the height variation from the earth barycentre is only due to the ellipticity of the orbit and to the fact that the perigee precedes along the ellipse itself with angular velocity [15].

$$\frac{d\omega_p}{dt} = \dot{\omega}_p = \frac{3}{4} n J_2 (1-e^2)^{-1} \left(\frac{R}{r}\right)^2 (1 - 5\cos^2 I) \quad . \tag{1.52}$$

In our case with $n \sim 1.2 \cdot 10^{-3} s^{-1}$, $i \sim 96^\circ$, $e = 0.002$ we find $\dot{\omega}_p \simeq 0.85 \cdot 10^{-6} s^{-1}$, which over a period of $\sim 5100\ s$ gives a displacement of $\sim 0.25^\circ$ per arc along the ellipse.

Now the maximum minus the minimum distance of the satellite from the earth center is

$$r_M - r_m = 2\ e\ r \cong 26.5 \quad km \tag{1.53}$$

increasing to $\sim 53\ km$ for $e = 0.004$, the maximum value of the eccentricity.

These two quantities are exchanged after the perigee has swept 180° along the ellipse, corresponding to ~ 750 revolutions. Accordingly we have in the average, at every revolution,

$$H \cong 30\ m \tag{1.54}$$

or up to 60 m in the extreme case, as we wanted to prove.

The conclusion is that loop points can be considered as particular cross-overs occurring more or less at the same altitude.

1.3.3 The loop checking procedure

As we have already seen in Section 2, for the case of loop points (cf. (12)) C and C_0 are very close to one another. Let us assume them to coincide, for a moment. Let us also make the hypothesis that we have the measurements along both orbits exactly at $C = C_0$. So we have, realistically, with good accuracy ($\sigma_0 = 3\ mE$),

$$\begin{aligned} &T_{xx}, \quad T_{yy}, \quad T_{zz}, \ T_{xz} \quad \text{in } C \\ &T_{x_0x_0}, \ T_{y_0y_0}, \ T_{zz}, \ T_{x_0z} \quad \text{in } C_0 \end{aligned} \tag{1.55}$$

The question is: how can we compare these quantities? One obvious answer is that, as far as the axis Z in the same in F and F_0, we must have

$$T_{zz}(C) \equiv T_{zz}(C_0) \ ; \tag{1.56}$$

unfortunately this is the only check we have at hand.

In fact from T_{xx}, T_{yy}, T_{zz} we could compute the 2^{nd} derivative in any direction of the (X, Y) plane; since however this is not the same as (X_0, Z_0), we cannot exploit this property[2].

On the other hand in the "horizontal" plane we have 2^{nd} derivatives in the four directions x, y, x_0, y_0 so that a linear relation has to hold among them. In fact, recalling the rotation formula for a 2^{nd} order tensor in the plane and inspecting Fig. 1.3, we see that, the angle between x and x_0 being $\pi - 2\alpha$,

$$\begin{cases} T_{x_0x_0} = T_{xx}\cos^2 2\alpha + 2T_{xy}\cos 2\alpha \sin 2\alpha + T_{yy}\sin^2 2\alpha \\ T_{y_0y_0} = T_{xx}\sin^2 2\alpha - 2T_{xy}\cos 2\alpha \sin 2\alpha + T_{yy}\cos^2 2\alpha \end{cases} \tag{1.57}$$

Equation (1.57) after eliminating T_{xy}, which is not available, gives the obvious relation

$$T_{x_0x_0} + T_{y_0y_0} = T_{xx} + T_{yy} \ . \tag{1.58}$$

This however is perfectly equivalent to (1.56), so that if we have already used the harmonicity property

$$T_{xx} + T_{yy} + T_{zz} = T_{x_0x_0} + T_{y_0y_0} + T_{z_0z_0} = 0 \ , \tag{1.59}$$

(1.58) cannot add any more constraint on the observed quantity.

The conclusion is that at loop points, beyond the usual traceless property (1.59) of M, only (1.56) is available for instrumental checks. This however is useful, since in

[2]Or better this property has to be exploited in order to perfectly align the two axes without loss of accuracy.

case of momentary failure at least the radial and the "horizontal" components can be discriminated.

Now we must consider that the instrument in general will measure at points A, B, A_0, B_0 different from $C = C_0$ so that we have to compute

$$\begin{cases} T_{zz}(C) = \lambda T_{zz}(A) + (1-\lambda) T_{zz}(B) \\ \\ T_{zz}(C_0) = \lambda_0 T_{zz}(A_0) + (1-\lambda_0) T_{zz}(B_0) \ . \end{cases} \tag{1.60}$$

The questions are:

a) What is the systematic error in (1.60), given that $AB \cong A_0B_0 \cong d = 8\ km$?

b) How does noise propagate from observations to $T_{zz}(C), T_{zz}(C_0)$?

As for the first question, we answer by a direct computation of $T_{zz}(C)$ comparing it with the result of (1.60) at a number of points.

φ_c, λ_c	$T_{zz}(A)$	$T_{zz}(B)$	$T_{zz}(C)$ (from (1.60))	$T_{zz}(C)$ (direct)
$2°, 2°$	-191.96	-185.62	-188.11	-189.46
$10°, 10°$	235.99	235.83	235.89	235.96
$20°, 20°$	-22.18	-23.54	-28.47	-26.31
$30°, 30°$	-78.09	-75.31	-76.41	-76.97
$40°, 40°$	523.81	540.03	533.63	530.39
$60°, 60°$	244.87	245.71	245.37	245.22
$70°, 70°$	-73.47	-70.53	-71.74	-72.25
$80°, 80°$	-67.77	-70.25	-69.40	-68.63

Table 1.1: Comparison between direct computation of $T_{zz}(C)$ and the results of (1.60): the values are in mE.

Our results are given in Table 1.1, from which we derive the reasonable guess that the systematic error is here well below the noise level.

As for the second question, we have clearly (assuming $T_{zz}(A)$ and $T_{zz}(B)$ uncorrelated)

$$\sigma^2 \left[T_{zz}(C)\right] = \left[\lambda^2 + (1-\lambda)^2\right] \sigma_0^2 \leq \sigma_0^2 \tag{1.61}$$

because

$$\lambda^2 + (1-\lambda)^2 \leq 1 \ , \qquad 0 \leq \lambda \leq 1 \ .$$

With a similar relation for $T_{zz}(C_0)$ we may conclude that

$$\sigma \left[T_{zz}(C) - T_{zz}(C_0)\right] \ \leq \sqrt{2}\sigma_0 \tag{1.62}$$

which is fairly good to test the functionality of the (zz) channel of the gradiometer.

Finally we want to be convinced that even if C, C_0 are separated in height[3] by $H \sim 100\ m$, the two points C, C_0 can be considered as coinciding with a systematic error negligible with respect to σ_0.

We can do that in two different ways: by computing the mean square value of T_{zzz} over a sphere at satellite's altitude or just by numerically checking the values of T_{zz} at some couple of points C, C_0 (cf. Fig. 1.1). We will follow both ways.

First of all take the anomalous potential T, from degree 13 on, and compute the 3^{rd} radial derivatives

$$T_{zzz} = -\frac{G_0}{R}\sum_{n=13}^{+\infty}\sum_{m=-n}^{n}(n+1)(n+2)(n+3)\left(\frac{R}{r}\right)^{n+4}T_{nm}Y_{n,m} \qquad (1.63)$$

$$\left(G_0 = \frac{\mu}{R^3} \cong 1.53\cdot 10^{-6}s^{-2}\right)\ .$$

Taking the average over the sphere gives

$$E\{T_{zzz}^2\} = \frac{1}{4\pi}\int\{T_{zzz}(r,\vartheta,\lambda)\}^2 dr = \frac{G_0^2}{R^2}\sum_{n=13}^{+\infty}(n+1)^2(n+2)^2(n+3)^2p^{2n+8}C_n(T) \quad (1.64)$$

where, according to Kaula's rule ([15])

$$p = \frac{R}{r} \cong 0.962281$$

$$C_n(T) \cong \sum_{m=-n}^{n}T_{nm}^2 \cong 2\cdot\frac{10^{-10}}{n^3}\ .$$

A rough, but efficient approximation of (1.64) is

$$E\{T_{zzz}^2\} \cong \frac{G_0^2}{R^2}2p^8 10^{-10}\sum_{n=13}^{+\infty}n^3p^{2n}\ . \qquad (1.65)$$

If we put $e^{-\alpha} = p^2$, we can further approximate

$$\sum_{n=13}^{+\infty}n^3p^{2n} \cong \int_{13}^{+\infty}t^3e^{-\alpha t}dt \cong 168\cdot 10^3\ ,$$

so that (1.65) yields

$$\sigma(T_{zzz}) = \sqrt{E\{T_{zzz}^2\}} \cong 1.24\cdot 10^{-15}s^{-2}m^{-1}\ . \qquad (1.66)$$

[3] As a matter of fact we expect to have $H \leq 50$ for every loop.

This shows that for a height difference of $H = 100\ m$

$$\sigma(T_{zz}(C) - T_{zz}(C_0)) \cong \sigma(T_{zzz}) \cdot H = 1.24 \cdot 10^{-13} s^{-2} \tag{1.67}$$

that is, as we promised, one order of magnitude smaller than σ_0.

To confirm our rough estimate given by (1.66) we have also tested a few incremental differences $H^{-1}\left[T_{zz}(C) - T_{zz}(C_0)\right]$ at different geographic locations and at satellite's altitude obtaining the results shown in Table 1.2.

φ, λ	$T_{zzz} = H^{-1}\left[T_{zz}(C) - T_{zz}(C_0)\right]$
$2°, 2°$	$+0.76\ 10^{-15}$
$10°, 10°$	$-0.91\ 10^{-15}$
$20°, 20°$	$+1.32\ 10^{-15}$
$30°, 30°$	$-0.46\ 10^{-15}$
$40°, 40°$	$-2.42\ 10^{-15}$
$60°, 60°$	$-1.28\ 10^{-15}$
$70°, 70°$	$+0.42\ 10^{-15}$
$80°, 80°$	$+0.12\ 10^{-15}$

Table 1.2 : Incremental differences T_{zzz} computed at several geographic locations: the values are in $s^{-2}\ m^{-1}$.

These values seem to agree very well with the estimate (1.66); incidentally their mean square value is $1.36 \cdot 10^{-15} s^{-2} m^{-1}$.

Concluding this Section we can say that in all cases of loop points, as well as for all cross-overs with H up to $1\ km$, we can use the equation

$$T_{zz}(C) = T_{zz}(C_0) \tag{1.68}$$

to check the functionality of the instrument, with a sensitivity of

$$\sigma\left[T_{zz}(C) - T_{zz}(C_0)\right] = \sqrt{2}\sigma_0\ .$$

We can observe that with $H = 1\ km$ we still have from (1.67) a sensivity of $1.24 \cdot 10^{-12} s^{-2}$ which is well below σ_0.

1.3.4 Cross-over conditions for arcs at different altitudes

When $H = \overline{CC_0} = 3\ km$, from (1.66) and (1.67) we see that

$$\sigma\left[T_{zz}(C) - T_{zz}(C_0)\right] = 3.72 \cdot 10^{-12} s^{-2}$$

which is not a negligible quantity with respect to the noise. Accordingly we cannot any more use (1.68) as a check, because the vertical gradient of T_{zz} is unknown and not negligible. So the question is whether we can still find some combination of the M components to be used as a check. The answer is that in principle it is possible, although it is not realistic in the actual configuration of the gradiometer because T_{xy}, T_{yz} are only very poorly known. Nevertheless we still believe it is interesting to realize how it could have been done; so in this Section we shall assume that the Marussi tensor M is known with independent components such that

$$\begin{cases} \sigma\left(T_{xx}\right) = \sigma\left(T_{yy}\right) = \sigma\left(T_{zz}\right) = \sigma\left(T_{xz}\right) = \sigma_0 \\ \\ \sigma\left(T_{yz}\right) = \sigma\left(T_{xy}\right) = \gamma\sigma_0 \end{cases} \tag{1.69}$$

under the hypothesis that γ is larger than 1 but not much (e.g. $\gamma = 3$).

Let us observe that

$$\begin{cases} \underline{e}_{x_0} = -\cos 2\alpha\ \underline{e}_x + \sin 2\alpha\ \underline{e}_y \\ \\ \underline{e}_x = -\cos 2\alpha\ \underline{e}_{x_0} + \sin 2\alpha\ \underline{e}_y\ , \end{cases} \tag{1.70}$$

as one can verify from Fig. 1.2. Therefore if we define the tensor linear functional

$$Q = \frac{\partial^2 T}{\partial x \partial x_0} \equiv \left(\underline{e}_x \cdot \nabla\right)\left(\underline{e}_{x_0} \cdot \nabla\right) T \tag{1.71}$$

we see that, by solving the differential operators in F, we can compute from M

$$Q = \frac{\partial}{\partial x}\left\{-\cos 2\alpha \frac{\partial}{\partial x} + \sin 2\alpha \frac{\partial}{\partial y}\right\} T \equiv -\cos 2\alpha \frac{\partial^2 T}{\partial x^2} + \sin 2\alpha \frac{\partial^2 T}{\partial x \partial y}\ . \tag{1.72}$$

Similarly if we resolve the differential operators in (1.71) in the frame F_0 we get

$$Q = -\cos 2\alpha \frac{\partial^2 T}{\partial x_0^2} + \sin 2\alpha \frac{\partial^2 T}{\partial x_0 \partial y_0}\ . \tag{1.73}$$

Since (1.71) is expressed in invariant terms, (1.72) and (1.73) do represent the same linear functional of T; the only difference being that it is computed by taking derivatives with respect to different axes, i.e. (1.72) is suitable to compute Q in A and B, while (1.73) is suitable for A_0 and B_0.

The first step here is to compute Q at C and C_0,

$$\begin{cases} Q(C) = \lambda Q(A) + (1-\lambda) Q(B) \\ \\ Q(C_0) = \lambda_0 Q(A_0) + (1-\lambda_0) Q(B_0) \end{cases} \tag{1.74}$$

with λ, λ_0 given by (1.45).

In order to compare these values we must further shift them to the mid-point K, what can be accomplished by formulas like

$$\begin{cases} Q^+(K) = Q(C) + \dfrac{\partial Q}{\partial z}(C)(H_K - H_C) \\ \\ Q^-(K) = Q(C_0) + \dfrac{\partial Q}{\partial z}(C_0)(H_K - H_{C_0}) \end{cases} \tag{1.75}$$

where obviously, referring to the example in Fig. 1.1

$$H_K - H_{C_0} = -(H_K - H_C) = \frac{H}{2} \ . \tag{1.76}$$

The sought check is therefore simply

$$Q^+(K) = Q^-(K) \ . \tag{1.77}$$

However the difficult point in (1.75) is: how can we obtain in a reliable way the two derivatives $\dfrac{\partial Q}{\partial z}(C)$, $\dfrac{\partial Q}{\partial z}(C_0)$?
This can be done as follows. Consider the quantity

$$V(A) = (\underline{e}_{x_0} \cdot \nabla)\,(\underline{e}_z \cdot \nabla)\,T = \frac{\partial^2 T}{\partial z \partial x_0}(A) \ ; \tag{1.78}$$

according to (1.70) this can be computed from M as

$$V(A) = -\cos 2\alpha \frac{\partial^2 T}{\partial x \partial x}(A) + \sin 2\alpha \frac{\partial^2 T}{\partial z \partial y}(A) \ . \tag{1.79}$$

Similarly we have in B

$$V(B) = -\cos 2\alpha \frac{\partial^2 T}{\partial z \partial x}(B) + \sin 2\alpha \frac{\partial^2 T}{\partial z \partial y}(B) \tag{1.80}$$

and due to the hypothesis of linearity of V along AB we can put at any C along that interval

$$\frac{V(A) - V(B)}{d} = \frac{\partial V}{\partial x}(C) = \frac{\partial^3 T}{\partial z \partial x \partial x_0}(C) = \frac{\partial Q}{\partial z}(C) \ , \tag{1.81}$$

which is the sought result.
The same, but exchanging the role of $\underline{e}_{x_0}$ and $\underline{e}_x$, can be done along (A_0B_0), providing the other derivative $V_0(A_0) = \dfrac{\partial^2 T}{\partial z \partial x}(A_0)$,

$$\frac{V_0(A_0) - V_0(B_0)}{d_0} = \frac{\partial^3 T}{\partial z \partial x \partial x_0}(C) = \frac{\partial Q}{\partial z}(C_0) \ . \tag{1.82}$$

So in principle the condition equation (1.77) can be used to check the functionality of the gradiometer. Naturally for this to be useful two basic conditions have to be satisfied; that measurement noise propagated to $(Q^+(K) - Q^-(K))$ would be small enough as to guarantee that errors of the order of $(5 \div 10)\sigma_0$ could be detected with a good significance level and that the hypotheses under which (1.77), (1.81), (1.82) are derived are satisfied with systematic errors not larger than the measurement noise. This point will be numerically demonstrated at the end of this Section.

But first we want to estimate the variance

$$\sigma^2 \left[Q^+(K) - Q^-(K) \right] \cong 2\sigma^2 \left[Q(K) \right] \ , \tag{1.83}$$

since we can reasonably assume that errors on the two crossing arcs are independent.

From (1.72) we can compute σ_Q^2 at points A and B

$$\sigma_Q^2 = \left(\cos^2 2\alpha + \gamma^2 \sin^2 2\alpha \right) \sigma_0^2 \ .$$

Moreover, recalling (1.61), the first of (1.74) gives

$$\sigma^2[Q(C)] \leq \sigma_Q^2 \ .$$

Now it is not difficult to see that, with realistic values, averaging over the unit sphere

$$E \left\{ \cos^2 2\alpha \right\} \cong 0.82$$

$$E \left\{ \sin^2 2\alpha \right\} \cong 0.18$$

so that we can put, in quadratic average,

$$\langle \sigma^2[Q(C)] \rangle \leq \langle \sigma_Q^2 \rangle = (0.82 + 0.18\gamma^2)\sigma_0^2 \tag{1.84}$$

On the other hand, from (1.81) we can compute

$$\sigma^2 \left(\frac{\partial Q}{\partial z} \right) = 2\frac{\sigma_V^2}{d^2}$$

and from (1.79), (1.80) reasoning as above

$$\langle \sigma_V^2 \rangle = (0.82 + 0.18\gamma^2)\sigma_0^2 \tag{1.85}$$

Summarizing we have

$$\sigma^2 \left[Q(K) \right] \cong \sigma^2 \left[Q(C) \right] + 2\frac{\sigma^2(V)}{d^2} \left(\frac{H}{2} \right)^2 + \left[\frac{\partial Q}{\partial z} \right]^2 \sigma_H^2 \ . \tag{1.86}$$

Since we can assume $\sigma_H \sim 3$ cm from GPS-GLONASS observations and on the same time typical values of $\left[\overline{\frac{\partial Q}{\partial z}}\right]$ are in the range of $10^{-15} s^{-2} m^{-1}$, we immediately see that the last term in (1.86) can be neglected. Therefore, recalling (1.84) and (1.85), we get from (1.86) the rough estimate

$$\sigma^2 \left[Q^+(K) - Q^-(K)\right] = 2\sigma^2 \left[Q(K)\right] \cong \left(2 + \frac{H^2}{d^2}\right) \left(0.82 + 0.18\gamma^2\right) \sigma_0^2 \ . \tag{1.87}$$

For instance with $\gamma = 3$ and $H = 2d = 16\ km$ we obtain the sensivity

$$\sigma \left[Q^+(K) - Q^-(K)\right] \cong 4\sigma_0 \tag{1.88}$$

which is still useful for a check OTF.

To conclude, regarding the fact that the hypotheses underlying formulas (1.77), (1.81), (1.82) do not hold systematic noise, we can numerically prove at a number of points that the computation of $(Q^+(K) - Q^-(K))$ introduces a bias smaller than the noise standard deviation (1.88). This is illustrated in Fig. 1.4 and Fig. 1.5 where $(Q^+(K) - Q^-(K))$ is computed, without any measurement noise, along one quarter of the parallel $\varphi = 60°$ and along the meridian $\lambda = 40°$.

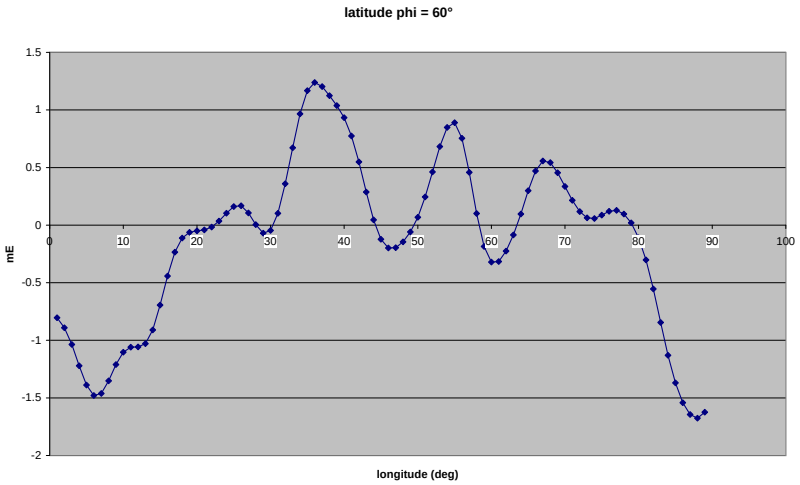

Figure 1.4: Differences $(Q^+(K) - Q^-(K))$ at points along the parallel $\varphi = 60°$.

1.3.5 The gradiometer check in the case of overlapping tracks

In Fig. 1.6 we illustrate the geometry of overlapping ground tracks and we immediately see that there are two distinct cases to be treated, depending on the fact that the difference in altitude between orbit arcs is $H < 1\ km$ or $H \geq 1\ km$.

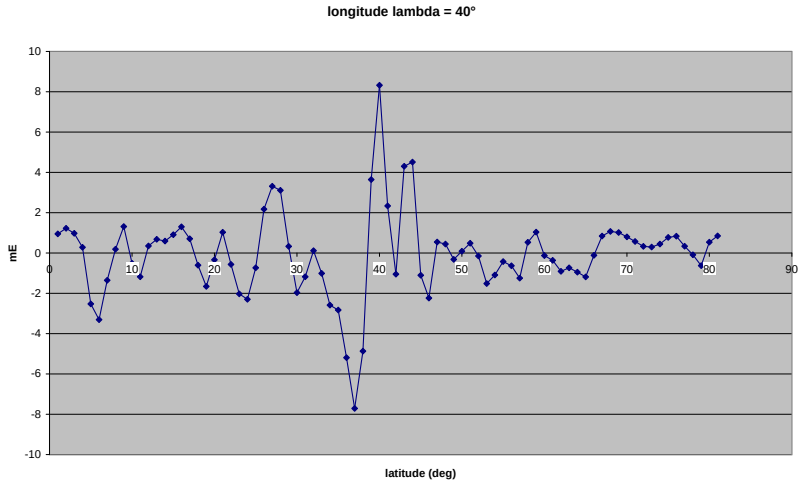

Figure 1.5 : Differences $(Q^+(K) - Q^-(K))$ at points along the meridian $\lambda = 40°$.

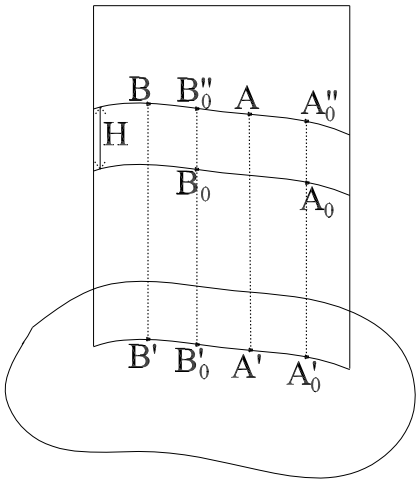

Figure 1.6 : Geometry of overlapping tracks.

As a matter of fact in the first case ($H < 1\ km$) we can assume the two tracks as coinciding. This happens because recalling (1.66) we can write the order of magnitude of the third derivatives as

$$O\left(T_{yyz}\right), O\left(T_{xxz}\right) < O\left(T_{zzz}\right) \cong 10^{-15} s^{-2} m^{-1} \ .$$

Therefore for these tracks we can just perform the along track linear interpolation putting for instance

$$T^+_{ii}(B_0) = \lambda T^+_{ii}(B) + (1-\lambda) T^+_{ii}(A) = T^-_{ii}(B_0) \qquad i = x, y, z \ . \tag{1.89}$$

On the other hand, when the separation in altitude between repeat tracks becomes larger, we still have at least one nice test to perform. In fact the T_{xx} component can

be shifted from one altitude to the other and then a simple linear interpolation test like (1.89) can be applied.

To transport for instance $T_{xx}(B_0)$ to $T_{xx}(B_0')$ we must put

$$T_{xx}(B_0') \cong T_{xx}^{+}(B_0) + T_{xxz}(B_0) \cdot H \ , \tag{1.90}$$

i.e. we need an estimate of $T_{xxz}(B_0)$. This can be obtained because we have accurate measurements of $T_{xz}(A_0)$, $T_{xz}(B_0)$, and so on, so that we can significantly put

$$T_{xxz} \cong \frac{T_{xz}(B_0) - T_{xz}(A_0)H}{d} \ . \tag{1.91}$$

This certainly gives us a negligible systematic error, while the noise inherited by $T_{xxz} \cdot H$ is just

$$\sigma\left(T_{xxz} \cdot H\right) = \sqrt{2}\ \sigma\left(T_{xz}\right) \frac{H}{d} \tag{1.92}$$

which is indeed acceptable at least up to $H \cong d$.

1.3.6 Conclusions

Three main conclusions can be drawn from the present study.

a) There is realistically a large number of cross-overs that differ in altitude by, say, less than 1 km, at least all loops are such that $H < 100\ m$; at all such cross-overs the condition of equality of 2^{nd} radial derivatives can be used as a check of the functionality of the gradiometer. We recall that T_{rr} can be computed with a small rotation in the orbital plane from T_{xx}, T_{zz}, T_{xz}, practically with no loss of accuracy.

b) If the components T_{xy}, T_{yz} would be available, with a better accuracy than what is allowed by the actual gradiometer configuration, even for deep cross-overs ($H > 3\ km$) we should be able to set up another cross-over check by computing T_{xx_0} from both arcs at one and the same point.

c) Closer analysis of the order of magnitude of 3^{rd} order derivatives and the fact that data might spread over a radial space of $\sim 24\ km$, shows that the problem of reducing data to a unique surface (sphere) in space should be more carefully reconstructed to make the space-wise approach completely consistent.

References

[1] A. Albertella, F. Migliaccio and F. Sansò: 1998, Contributions to the GOCE mission in the space-wise approach - Report 1 *GOCE Phase A1 Data Package*, Vol.2, GOC-ED-AI-0001, December 1998.

[2] A. Albertella, F. Migliaccio and F. Sansò: 1998, A contributions from space-wise approach to the assessment of instruments performance - Report 2 *GOCE Phase A1 Data Package*, Vol.2, GOC-ED-AI-0001, December 1998.

[3] Albertella, A., F. Sacerdote, F. Sansó: 1999, Progress Report 3, GOCE WP 2320 Science Performances, Phase A2.

[4] Albertella, A., F. Sansó, N. Sneeuw: 1999, Band-limited functions on a bounded spherical domain: the Slepian problem on the sphere. Submitted to Journal of Geodesy, in print.

[5] Arabelos, D. and C.C.Tscherning: 1990, Simulation of regional gravity field recovery from satellite gravity gradiometer data using collocation and FFT. Bulletin Geodesique, Vol. 64, pp. 363-382.

[6] Arabelos, D. and C.C.Tscherning: 1995, Regional recovery of the gravity field from SGG and Gravity Vector data using collocation. J.Geophys. Res., Vol. 100, No. B11, pp. 22009-22015.

[7] Arabelos, D. and C.C.Tscherning: 1998, Calibration of satellite gradiometer data aided by ground gravity data. Journal of Geodesy, Vol. 12, no. 11, pp . 617 - 625.

[8] Arabelos, D. and C.C.Tscherning: 1999, Gravity field recovery from airborne gravity gradiometer data using collocation and taking into account correlated errors. Phys. Chem. Earth (A), Vol. 24, No. 1, pp. 19-25.

[9] ASI: 1998, SAGE Phase A Final Report (Albertella and Migliaccio eds.), Agenzia Spaziale Italiana.

[10] Balmino G., Perosanz F., Rummel R., Sneeuw N., Suenkel H.: 1998, CHAMP, GRACE and GOCE: Mission Concepts and Simulations, II Joint Meeting of the International Gravity Commission and the International Geoid Commission, Trieste, Italy, in print.

[11] Bassanino M., Migliaccio F., Sansó F.: 1996, The Aristoteles mission: problems related to data distribution. "Ricerche di geodesia , topografia e fotogrammetria" n. 12 "Aristoteles - Step - Gem", DIIAR - Politecnico di Milano, Milano.

[12] Betti B. and Sansò F.: 1989, The integrated approach to satellite geodesy, Lecture notes in earth sciences n. 25, "Theory of satellite geodesy and gravity field determination" (Sansò and Rummel eds.), Springer-Verlag.

[13] ESA: 1998, European Views on Dedicated Gravity Field Missions: GRACE and GOCE, ESD-MAG-REP-CON-001, ESA, May 1998.

[14] ESA: 1999, GOCE Phase A Preliminary Requirements Review Presentation, ESA, June 1999.

[15] Kaula W.M.: 1966, Theory of Satellite Geodesy, Blaisdell Publishing Company Waltham, Massachusetts-Toronto-London.

[16] Migliaccio F., Sansó F.: 1989, Data processing for the Aristoteles Mission, Proc. Italian Workshop on the European Solid Earth Mission Aristoteles, Trevi, Italy.

[17] Rummel R.: 1986, Satellite gradiometry. Lecture Notes in Earth Sciences (H. Suenkel ed.), Vol. 7, Springer-Verlag.

[18] Rummel R., Van Gelderen M., Koop R., Schrama E., Sansò F., Brovelli M., Migliaccio F., Sacerdote F.: 1993, Spherical harmonic analysis of satellite gradiometry. *Netherlands Geodetic Commission, Publications on Geodesy, New Series*, no. 39, Delft.

[19] Sacerdote F., Sansò F.: 1989, Some problems related to satellite gradiometry. *Bulletin Geodesique*, vol. 63, n. 4, pp. 405-415.

[20] Sansó, F. and S. Usai: 1996, The new GEM ESA mission: data reduction theory and first simulations. Ricerche di geodesia, topografia e fotogrammetria n. 12 "Aristoteles, STEP, GEM", DIIAR, Politecnico di Milano.

[21] Sansó, F. and S. Usai: 1996, The new GEM ESA mission: interpolation errors, commission errors and errors due to holes in the data. Ricerche di geodesia, topografia e fotogrammetria n. 12 "Aristoteles, STEP, GEM", DIIAR, Politecnico di Milano.

[22] Sneeuw, N., R. Dorobantu, C. Gerlach, J. Mueller, H. Oberndorfer, R. Rummel, R. Koop, P. Visser, P. Hoyng, A. Selig, M. Smit: 1998, Simulation of the GOCE Gravity Field Mission. Proc. IV Hotine - Marussi Symp. on Mathematical Geodesy, Trento, in print.

[23] Tscherning, C.C., P.Knudsen and R.Forsberg: 1994, Description of the GRAVSOFT package. Geophysical Institute, University of Copenhagen, Technical Report, 1991, 2. Ed. 1992, 3. Ed. 1993, 4. ed, 1994.

[24] Tscherning, C.C., F.Rubek and R.Forsberg: 1998, Combining Airborne and ground Gravity using Collocation. In: Forsberg,R., M.Feissel, R.Dietrich (Eds): Geodesy on the Move. Proceeding IAG Scientific Assembly, Rio de Janeiro, Sept. 1997 ,IAG Symp. Vol. 119, pp.18-23, Springer-Verlag.